

Results from the Wide Angle Search for Planets Prototype (WASP0) I: Analysis of the Pegasus Field

Stephen R. Kane¹, Andrew Collier Cameron¹, Keith Horne¹, David James^{2,3},
Tim A. Lister¹, Don L. Pollacco⁴, Rachel A. Street⁴, Yiannis Tsapras⁵

¹*School of Physics & Astronomy, University of St Andrews, North Haugh, St Andrews, Fife KY16 9SS, Scotland*

²*Department of Physics & Astronomy, Vanderbilt University, Nashville, TN 37235, USA*

³*Laboratoire d'Astrophysique, Observatoire de Grenoble, BP 53, F-38041, Grenoble, Cedex 9, France*

⁴*School of Mathematics and Physics, Queen's University, Belfast, University Road, Belfast, BT7 1NN, Northern Ireland*

⁵*School of Mathematical Sciences, Queen Mary University of London, Mile End Road, London, E1 4NS, UK*

14 June 2018

ABSTRACT

WASP0 is a prototype for what is intended to become a collection of wide-angle survey instruments whose primary aim is to detect extra-solar planets transiting across the face of their parent star. The WASP0 instrument is a wide-field (9-degree) 6.3cm aperture F/2.8 Apogee 10 CCD camera (2Kx2K chip, 16-arcsec pixels) mounted piggy-back on a commercial telescope. We present results from analysis of a field in Pegasus using the WASP0 camera, including observations of the known transiting planet around HD 209458. We also present details on solving problems which restrict the ability to achieve photon limited precision with a wide-field commercial CCD. The results presented herein demonstrate that millimag photometry can be obtained with this instrument and that it is sensitive enough to detect transit due to extra-solar planets.

Key words: methods: data analysis – stars: variables – stars: individual (HD 209458) – planetary systems

1 INTRODUCTION

In the search for extra-solar planets, indirect methods have been used to detect the more than 100 planets discovered thus far (e.g., Mayor & Queloz (1995); Marcy & Butler (1996); Delfosse et al. (1998)). Of the indirect methods, the use of transits (Borucki, Scargle, & Hudson 1985) is rapidly developing into a strong and viable means to detect extra-solar planets. A transit occurs when the apparent brightness of a star decreases temporarily due to an orbiting planet passing between the observer and the stellar disk, leaving a photometric signature of the planet in the lightcurve of the parent star.

The radial velocity surveys have shown that roughly 7% of sun-like (F5–K5) stars in the solar neighbourhood are orbited by a jupiter-mass companion in the orbital range 0.035–4.0 AU. Moreover, 0.5%–1% of sun-like stars in the solar neighbourhood have a jupiter-mass companion in a 0.05 AU (3–5 day) orbit (Lineweaver & Grether 2003). If the orbital plane of these “hot jupiters” is randomly oriented, approximately 10% (averaged over all sun-like stars) will transit the face of their parent star as seen by an observer. Thus roughly 1 sun-like star in 1000 will produce

detectable transits due to an extra-solar planet. Since this transit method clearly favours large planets orbiting their parent stars at small orbital radii, a large sample of stars must be monitored in order to detect statistically meaningful numbers of transiting planets.

Over the entire sky, roughly 1000 stars brighter than 13th magnitude should be exhibiting lightcurve dips due to transiting jupiter-mass extra-solar planets. The photometric accuracy required to reliably detect a transiting planet in a 3–5 day orbit is considerably higher than that typically necessary for CCD photometry of variable stars, since starlight dims by about 1% for a few hours during each orbital period. Because thousands of lightcurves must be studied to find one that exhibits transits, a signal-to-noise (S/N) ratio of at least 6–10 is needed to reliably detect the transits. Since the cost of detecting transiting planets can be dominated by the cost of a CCD, it is useful to test if commercial large-format CCD cameras are able to achieve milli-magnitude accuracy on 1 hour timescales, and thus sufficient accuracy to be able to reliably detect transits. Success would show that a large number of similar cameras could be relatively cheaply deployed in order to monitor the entire sky for transits.

We present first results from the Wide Angle Search

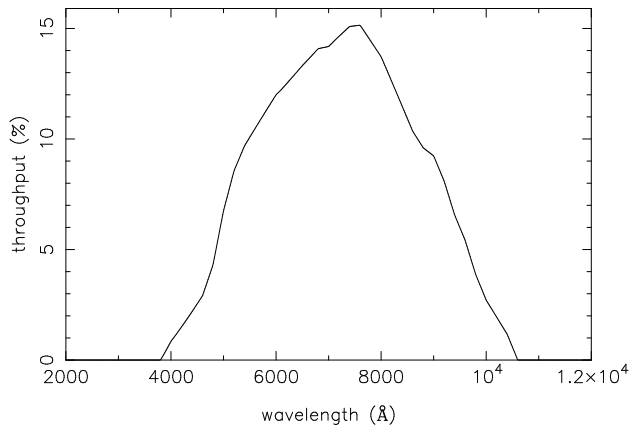


Figure 1. CCD response of WASP0.

for Planets prototype (hereafter WASP0), a wide-field instrument used to search for planetary transits. We describe the data reduction methods and show that the required accuracy can be achieved with this instrument provided that sources of systematic errors are treated appropriately. Observations of the known transiting planet, HD 209458b, are presented as well as a selection of other stars in the field which exhibit transit-like lightcurves. The WASP0 instrument was developed as a proof-of-concept instrument similar to Vulcan (Borucki et al. 2001) to search for planetary transits, and as a precursor to SuperWASP (Street et al. 2003), a more advanced instrument that has recently been constructed on La Palma, Canary Islands.

2 WASP0 HARDWARE

WASP0 is an inexpensive prototype for SuperWASP, whose primary aim is to detect transiting extra-solar planets. The WASP0 instrument is a wide-field (9-degree) 6.3cm aperture F/2.8 Nikon camera lens, Apogee 10 CCD detector (2K × 2K chip, 16-arcsec pixels) which was built by Don Pollacco at Queen’s University, Belfast. Calibration frames were used to measure the gain and readout noise of the chip and were found to be $15.44 e^-/ADU$ and 1.38 ADU respectively. Images from the camera are digitized with 14-bit precision giving a data range of 0–16383 ADUs. Figure 1 shows the expected WASP0 sensitivity with the main losses resulting from the CCD quantum efficiency. The instrument uses a clear filter which has a slightly higher red transmission than blue.

During its observing run on La Palma, Canary Islands, WASP0 was mounted piggy-back on a commercial 8-inch Celestron telescope with a German equatorial mount. More recently at Kryoneri, Greece, WASP0 was mounted on a 10-inch Meade with a fork equatorial mount.

3 OBSERVATIONS

WASP0 has had two successful observing runs at two separate sites. The first observing run was undertaken on La Palma, Canary Islands during 2000 June 20 – 2000 August 20. The second observing run took place at Kryoneri, Greece

Table 1. Field centres of WASP0 observations (J2000.0)

Field	RA	Dec
Pegasus	22 03 11	18 53 04
Draco	17 40 00	47 55 00
Hyades	04 24 40	17 00 00

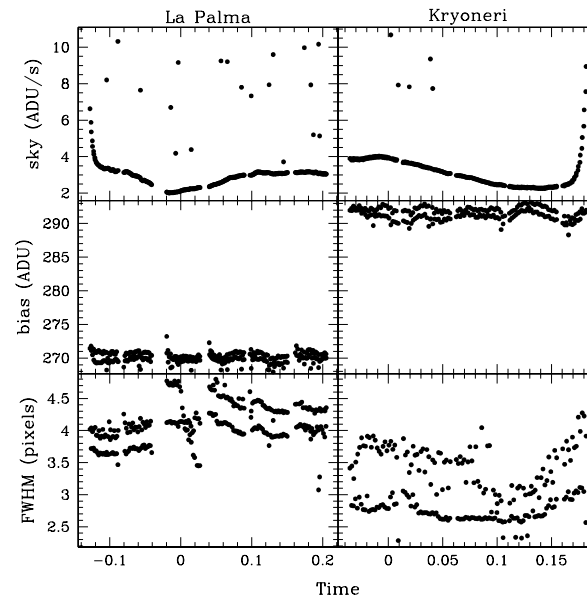


Figure 2. Comparison of observing sites, La Palma and Kryoneri. The time is expressed as fractional days since local midnight.

between 2001 October – 2002 May. In order to monitor sufficient numbers of stars for successful planetary transit detection, a wide field needs to be combined with reasonably crowded star fields. Observations on La Palma concentrated on a field in Draco which was regularly monitored for two months. More recent observations from Greece have largely been of the Hyades open cluster along with further observations of the Draco field. Observations of the Draco field from La Palma were interrupted on four occasions when a planetary transit of HD 209458 was predicted. On those nights, a large percentage of time was devoted to observing the HD 209458 field in Pegasus. This paper details results from the Pegasus field while the results from the Draco and Hyades observations will be published elsewhere. The fields centre for each field monitored by WASP0 is shown in Table 1.

During the night, the WASP0 camera was operated via a series of Visual Basic scripts which automated the observations and collected both science and calibration frames. The dead time between exposures was typically the same as the readout time for the chip (approximately 8 seconds) since the camera is ready as soon as readout is complete. With the exception of the Pegasus field observations, science frames generally alternated between 20s and 120s to extend the dynamic range so that brighter stars saturated in the longer exposure would be unsaturated in the shorter exposure.

Figure 2 presents a comparison of the two observing sites used for WASP0 observations. Each of the nights are dark nights and the data are from observations of the same field. The sky brightness is quite similar between the two

sites, though light pollution from the nearby city of Corinth combined with the cloud-producing bay make observations from Kryoneri towards the east difficult. The points of high sky brightness shown are likely caused by the observer’s torch shining too close to the WASP0 field of view. The middle panels show that the bias level remains fairly constant and drifts over a range of 10 ADU in the course of each night. The point-spread function is defined mainly by camera optics rather than atmospheric seeing due to the large pixel size. Hence the FWHM is often larger in the 120s than in the 20s exposures due to smearing of the stellar profiles arising from wind shake and tracking errors. This effect can be clearly seen in the lower panels of Figure 2.

A problem encountered with observations from La Palma resulted from the use of the German equatorial mount. A well-known flaw of the German equatorial mount is that it is impossible to sweep continuously from east to west in one movement. As the telescope nears the meridian, the telescope must be swung around to the other side of the mount and the target must be re-acquired so that observations can continue to the west. The result of this, besides interruptions to the observing, is that frames in the second half of the night are rotated 180° relative to frames obtained in the first half. The fork equatorial mount used at Kryoneri presented no such problem, allowing continuous observations of targets.

4 DATA REDUCTION

During the first two months of WASP0 observations, nearly 150 Gigabytes of data were obtained. A data pipeline has been developed to reduce this dataset with a high level of automation. The reduction of wide-field optical images requires special care since there are many spatially dependent aspects which are normally assumed to be constant across the frame. The airmass and even the heliocentric time correction vary significantly from one side of the frame to the other. The most serious issues arise from vignetting and barrel distortion produced by the camera optics which alter the position and shape of stellar profiles. This tends to be particularly severe in the corners of the image (see Figure 3). Many of these issues are compounded in the 2000 La Palma data due to the image rotation caused by the use of the German equatorial mount.

These problems have been largely solved through the implementation of an astrometric fit which uses both the Tycho-2 (Høg et al. 2000) and USNO-B (Monet et al. 2003) catalogues. Rather than fit the variable point-spread function (PSF) shape of the stellar images, weighted aperture photometry is used to compute the flux centred on catalogue positions. Post-photometry calibrations are then applied to remove nightly trends from the data. These steps will now be described in greater detail.

4.1 Point-Spread Function Profiles

The images acquired with WASP0 are normally slightly defocussed so that the point-spread functions have a FWHM of a few pixels. Spreading out the starlight in this way increases the sky background against which each star must be measured. The hope is that this sacrifice of statistical

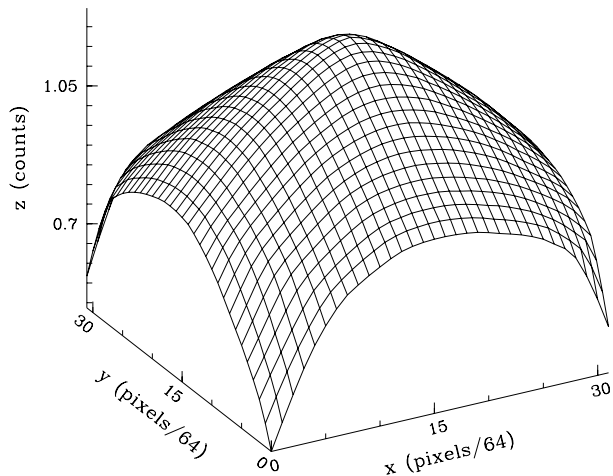


Figure 3. Vignetting pattern across the surface of the frame as measured from the normalised median flat-field.

accuracy will result in reduced systematic errors that could arise from undersampling of stellar images by the 15-arcsec pixels.

Due to the wide-field and the optics of the camera, the shape of the PSF varies with a roughly radial dependence. The photometry package used most extensively was a modified version of DoPHOT (Schechter, Mateo, & Saha 1993), the most important modification being the use of the flat-field to calculate a more adequate noise model for the image. However, DoPHOT still used the weighted average of the PSF shape parameters when subtracting stars from the image and so the shape parameters were dominated by the large number of circular shaped stars in the centre of the frame. Figure 4 (left) shows an sample of stars from a WASP0 image with the central star being close to the centre of the image. Figure 4 (right) shows the same stars after the spatially-independent PSF model has been subtracted. It has also been discovered that there is a strong colour dependence which is strengthened by the use of a clear filter during observations.

4.2 Frame Classification and Calibration

WASP0 FITS headers contain minimal information, so an automated frame classifier was developed to identify the nature of the frames. Identification is achieved by statistical measurements and the frames are classified as one of bias, flat, dark, image, or unknown. Master calibration frames are then generated after quality control checks are performed which count the number of saturated pixels.

Since the WASP0 camera has no overscan region, bias frames were taken at regular intervals during the night. However, it was discovered that a dead column on the CCD could effectively be used as an overscan region and so the median value of this strip is subtracted from the frame. Sky flats were used to flat-field the science frames but were difficult to obtain due to the 40% vignetting in the corners relative to the centre and the short exposures needed to avoid saturation. A shutter time correction map is applied to the master flat to take into account the radial and azimuthal structure

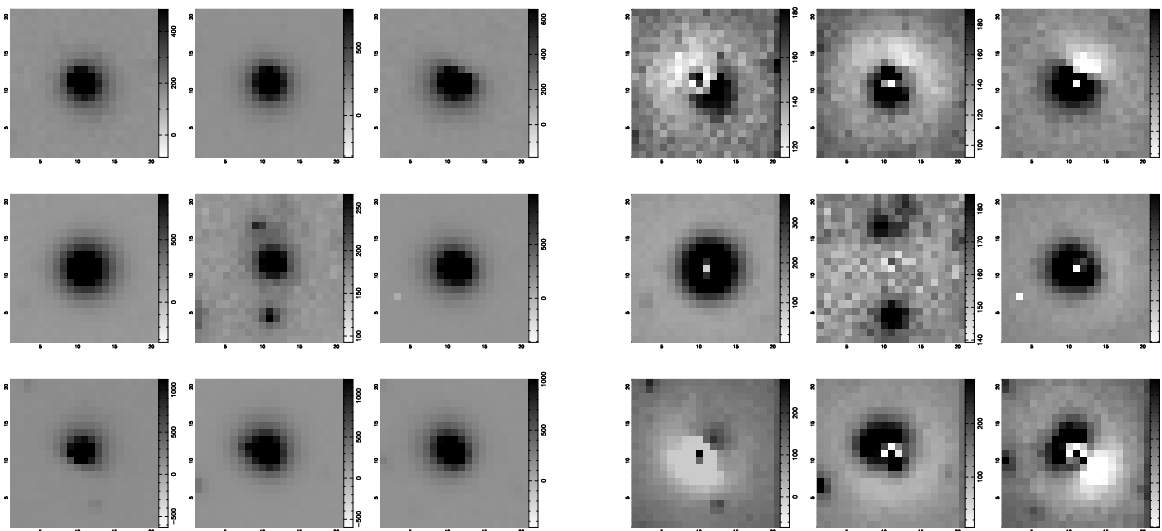


Figure 4. A sample of star images demonstrating the shape of the PSF in the centre of the image and around the edges. The figure on the right shows the same stars after a model PSF has been subtracted.

caused by the shutter blades on exceptionally short exposures.

4.3 Astrometry

The first step in the astrometry procedure is to create an object list from an image with rough aperture magnitudes using the Starlink `Extractor` program, which is derived from `SExtractor` (Bertin & Arnouts 1996). The coordinates of the nominal field centre are used to extract a subset of the Tycho-2 catalogue, covering an area slightly wider than the camera’s field of view. Star coordinates in the tangent plane are computed from the Tycho-2 catalogue by gnomonic projection, after transformation of the catalogue coordinates from mean to observed place. The gnomonic projection uses initial estimates of the optical axis location on the sky and the barrel distortion coefficient.

The WASP0 astrometry software automatically cross-identifies a few dozen bright stars present on both lists, and computes an initial 4-coefficient astrometric solution which describes the translation, scaling, and rotation of the CCD coordinates in the tangent plane. This solution allows the cross-identification of many more stars found by `Extractor` with their Tycho-2 counterparts. The locations of the optical axis on the sky and on the CCD are refined iteratively, together with the barrel-distortion coefficient, using the downhill simplex algorithm. At each iteration a new 4-coefficient astrometric fit is computed. Once the solution has converged, a final 6-coefficient fit is computed, which corrects for any small amount of image shear that may be present.

Figure 5 shows the number of stars used in computing the final astrometric fit and the associated rms error. On frames of high sky background, especially noticeable during morning twilight, faint stars are excluded from the fit resulting in a slightly improved rms. Once the solution has been computed, the much deeper USNO-B catalogue is read and the object positions within the cameras’s field of view are transformed to CCD x, y positions and are written to

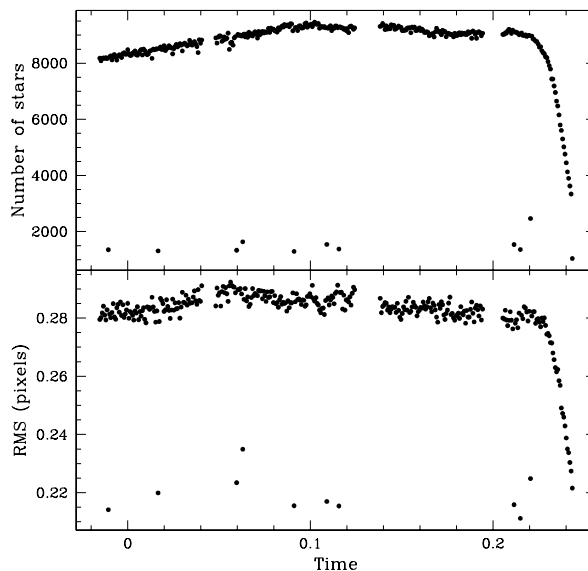


Figure 5. Number of stars used for the astrometric fit and the RMS of the fit. The time is expressed as fractional days since local midnight.

a catalogue along with the RA and Dec coordinates, the heliocentric time correction, and the airmass. This output catalogue is now ready for the photometry stage.

4.4 Photometry

Using the USNO-B catalog stars, we excluded circular regions with radii depending on star brightness to define a skymask. The curvature of the sky in the wide-field frames presented a new problem in determining local sky values and hence producing adequate photometry. This was solved through a sky fitting routine which fits a quadratic surface

to the image excluding circles of tunable radius around the known positions of stars from the catalogue. In this sense, the deeper USNO-B catalogue resulted in a great improvement of the fit since faint stars which would artificially raise the sky level are also excluded when fitting the surface. An iterative process then ensues during which the sky fit is refined by applying a sigma-clip to remove cosmic rays and other outliers. Once the final image of the quadratic surface is produced, the pixels removed from the fit are used to create a sky rejection mask.

The aperture photometry routine then computes the flux in a circular aperture of tunable radius centred on the predicted positions of all objects in the catalogue. The sky background is computed beyond a larger exclusion radius after subtracting the quadratic sky surface and excluding pixels defined in the sky rejection mask. Since the aperture is centred on the actual star position, the weights assigned to pixels lying partially outside the aperture are computed using a Fermi-Dirac-like function. This is tuned to drop smoothly from 1.0 at half a pixel inside the aperture boundary to 0.0 at half a pixel outside the boundary. The weights of these edge pixels are renormalised to ensure that the effective area of the aperture is πr^2 where r is the aperture radius in pixels. This acts to “soften” the edges of the aperture to take into account the large pixel size. The resulting photometry still contains time and position dependent trends which we removed by post-photometry calibration.

4.5 Post-Photometry Calibration

The post-photometry calibration of the data is achieved through the use of a post-photometry calibration code. This constructs a theoretical model which is then subtracted from the data leaving residual lightcurves. The residuals are then fitted via an iterative process to find systematic correlations in the data.

As well as fitting for time dependence, airmass, and colour; the theoretical model can optionally include a polynomial fit of degree ≤ 3 to take spatial variance into account. A theoretical model for the predicted instrumental magnitude of star s consisting of time $\Delta m_t(t)$, colour $\Delta m_c(t)$, airmass Δm_a , and quadratic spatial dependence takes the form

$$\begin{aligned}
 m(s, t) &= m_s(s) \\
 &+ \Delta m_t(t) + \Delta m_c(t) \eta_c(t) + \Delta m_a \eta_a(s, t) \\
 &+ \Delta m_x(t) \eta_x(s, t) + \Delta m_y(t) \eta_y(s, t) \\
 &+ \Delta m_{xx}(t) \eta_{xx}(s, t) + \Delta m_{yy}(t) \eta_{yy}(s, t) \\
 &+ \Delta m_{xy}(t) \eta_{xy}(s, t)
 \end{aligned} \tag{1}$$

where $m_s(s)$ is the instrumental magnitude of star s , the Δm terms represent magnitude corrections for various systematic errors, and the η terms are the corresponding dimensionless basis functions. For example, $\Delta m_t(t)$ accounts for a time-dependent sensitivity. The extinction coefficient Δm_a scales the basis function

$$\eta_a(s, t) = a(s, t) - a_0.$$

to correct the airmass $a(s, t)$ for star s at time t to a fiducial airmass $a_0 = 1$. Similarly, the colour term $\Delta m_c(t)$ corrects to a fiducial colour index, and the spatial terms correct to the centre of the chip. Iterations of the chosen calibration

model are considered to have converged if the magnitude difference in applying the model is less than an arbitrarily small value (usually 10^{-6}). RMS vs magnitude plots are available to evaluate the improvement by applying the model and the de-trended lightcurves can then be further analysed for variable and transit signatures.

4.6 Transit Detection Algorithm

The final stage in the WASP0 data processing is the search for planetary transit signatures in the stellar lightcurves. There have been a variety of methods (eg., DeFay, Deleuil, & Barge (2001); Doyle et al. (2000); Kovács, Zucker, & Mazeh (2002)) discussed on the topic of automating transit searches. Two of the important issues for such methods are the reduction of computational time to a reasonable value and the optimisation of the model to avoid false positive detections. The method used here is a matched-filter algorithm which generates model transit lightcurves for a selected range of transit parameters and then fits them to the stellar lightcurves.

The transit model used for fitting the lightcurves is a truncated cosine approximation with four parameters: period, duration, depth, and the time of transit midpoint. The search first performs a period sweep with a fixed duration over all the lightcurves. The advantage of fixing the duration to a reasonable value and then scanning for multiple transits is that it dramatically reduces the number of false positive detections by avoiding single dip events. The search is refined by performing a duration sweep on those stars which are fitted significantly better by the transit model compared with a constant lightcurve model. A transit S/N statistic is calculated for each lightcurve based on the resulting reduced χ^2 and $\Delta\chi^2$. The folded lightcurves of these stars are examined individually to assess the fit of the transit model. The transit detection algorithm is discussed in more detail in Section 5.3.

5 RESULTS

Presented in this section are the results from four nights of monitoring the Pegasus field. These nights were planned to coincide with predicted transits by the known extrasolar planet orbiting HD 209458 (Charbonneau et al. 2000; Henry et al. 2000).

5.1 Photometric Accuracy

The upper panel of Figure 6 shows the RMS vs magnitude diagram achieved by the aperture photometry previously described after correction of systematic errors. The lower panel shows the same RMS accuracy divided by the predicted accuracy for the CCD. The data shown include around 7800 stars at 311 epochs from a single night of WASP0 observations and only includes those stars for which a measurement was obtained at 90% of epochs. The night in question was 8th August, 2000 during which 50 second exposures were taken and, although the night was clear, was during bright time. The location of HD 209458 on the diagram is indicated by a 5-pointed star. The black curve indicates the theoretical noise limit with the $1-\sigma$ errors being shown by the dashed

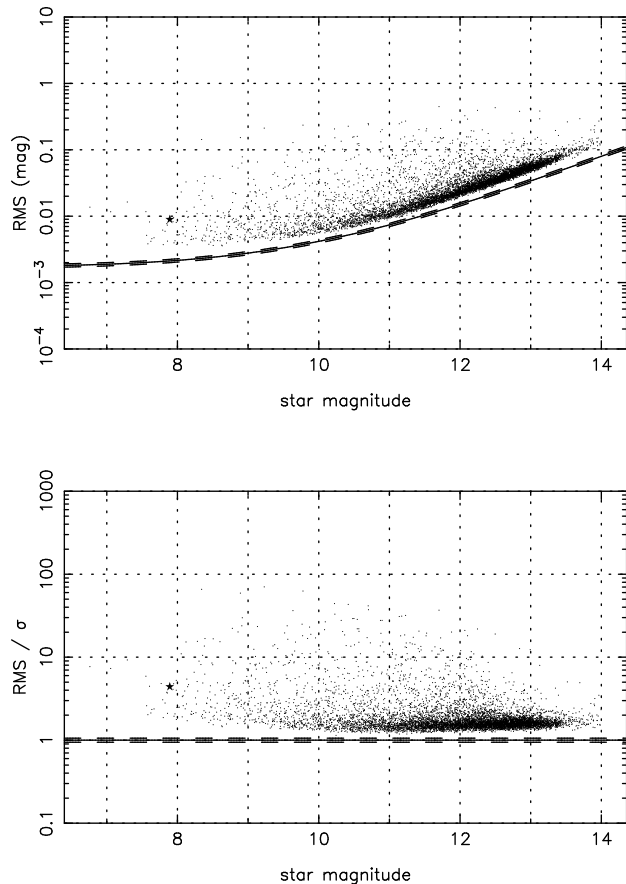


Figure 6. Photometric accuracy vs magnitude diagram from the night of 8th August, 2000 with the location of HD 209458 shown as a 5-pointed star. The upper panel shows the RMS accuracy in magnitudes in comparison with the theoretical accuracy predicted based on the CCD noise model. The lower panel is the ratio of the observed RMS divided by the predicted accuracy.

lines either side. It should be noted that this theoretical noise limit assumes that optimal extraction using PSF fitting has been used, with a CCD noise model given by

$$\sigma^2 = \left(\frac{\sigma_0}{F(x, y)} \right)^2 + \frac{\mu(x, y)}{G F(x, y)} \quad (2)$$

where σ_0 is the readout noise (ADU), G is the gain (e^-/ADU), and $F(x, y)$ is the flat-field.

There is a notable offset between the RMS accuracy and the predicted accuracy shown in Figure 6 due to sky photon noise and scintillation noise. It is also worth noting that a number of stars exhibit a magnitude jump, which occurs when the field is rotated 180° , due to the change in shape of the PSF. This is particularly severe in the case of faint stars with bright neighbours. Nonetheless, an RMS scatter of 4 millimag is achieved for stars brighter than magnitude 9.5, rising smoothly to 0.01 mag at magnitude 11.0. This demonstrates that WASP0 is able to achieve the millimag accuracy needed in order to be sensitive to planetary transits due to extra-solar planets.

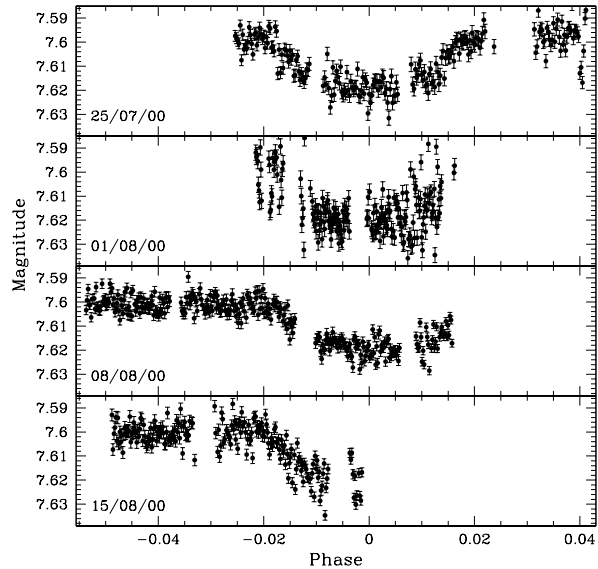


Figure 7. HD 209458 lightcurves from four nights of Pegasus observations showing the transit of the parent star by the planet HD 209458b.

5.2 HD 209458

The field in Pegasus containing HD 209458 was monitored closely on four nights of predicted transits; 25th July, 1st August, 8th August, and 15th August, 2000. Each of these nights were relatively clear with the exception of 1st August which was frequently interrupted by cloud. The exposure times on each of these nights was 5, 30, 50, and 50 seconds respectively. In order to match with the frames from the second night, the 5 second frames were rebinned in groups of six to create equivalent 30 second exposures.

Figure 7 shows the HD 209458 lightcurves on each of the four nights in which the planetary transit is clearly visible. This successfully tests the capability of the WASP0 system to detect small-scale deviations in stellar lightcurves.

5.3 Planetary Transit Search

The field monitored in Pegasus provides an ideal test dataset for the transit detection algorithm described earlier, since there is known to be at least one transiting planet in the field. Passing the lightcurves through the algorithm with a period range of between 3 and 4 days and with a fixed duration of 3 hours produces the plots shown in Figure 8, with the location of HD 209458 on each diagram indicated by a 5-pointed star. It can be seen that HD 209458 is well separated from the majority of stars in each of these diagrams. These results are of course already biased towards a HD 209458 planet detection since we only observed the star on nights on which a transit was predicted to occur.

Each of the four plots shows various star characteristics plotted against the transit S/N, S_W , which is defined as

$$S_W^2 = \frac{\Delta\chi^2}{\chi_{\min}^2/(N-f)} \quad (3)$$

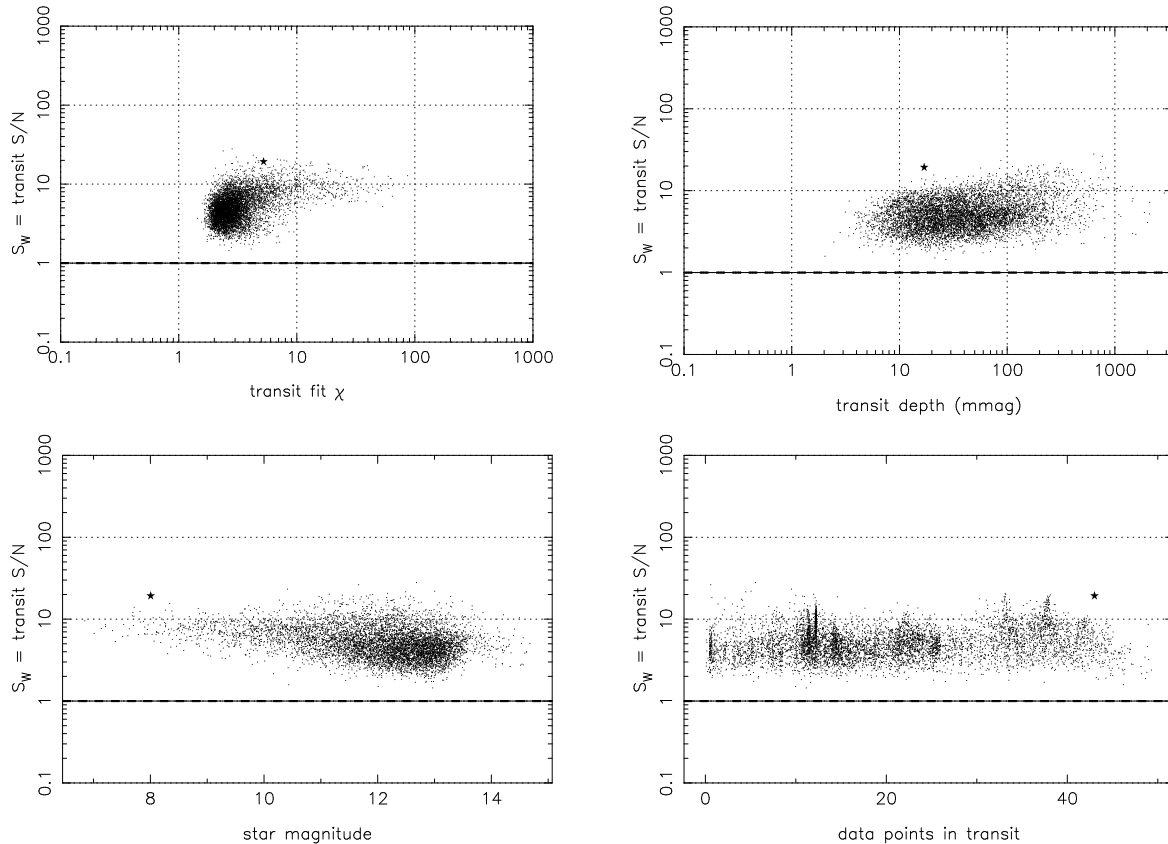


Figure 8. Results of a passing the data through the transit detection algorithm with a period range of between 3 and 4 days with a fixed duration of 3 hours. Each of the plots are plotted against the transit S/N which measures the “goodness-of-fit” of each staller lightcurve to a transit model.

where N is the number of data points, f is the number of free parameters, and $\Delta\chi^2$ is given by

$$\Delta\chi^2 = \chi_{\text{constant}}^2 - \chi_{\text{transit}}^2.$$

The errors in the individual lightcurves are rescaled by a factor that forces the $\chi_{\text{min}}^2/(N - f)$ for each lightcurve to be equal to unity. The S_W statistic shown in equation 3 is used consistently throughout the transit detection algorithm, including the first pass in which the transit duration is fixed. As can be seen from the plots in Figure 8, this transit S/N is an effective means for sifting transit candidates from the data.

An arbitrary S_W (transit S/N) threshold may be used to isolate stars with possible transits for further analysis. In Figure 8, for example, stars which yield $S_W > 10$ would be an ideal group to investigate further. For stars with multiple transits, the folded lightcurves may be examined which also gives a quick estimate of the transit depth. Using colour information from the Tycho-2 and USNO-B catalogues, these transit depths can be translated into Jupiter radii and hence it can be determined whether the star may be classified as a transit candidate and suitable for further follow-up.

The transit model was refined for HD 209458 by allowing the transit duration vary between 2 and 4 hours and expanding the period range to between 2 and 5 days with much higher time resolution. These results can be seen in Figure 9. The fit parameters for the planetary transit of

HD 209458 are a depth of $\Delta m = 1.7\%$, a duration of $\Delta t = 2.790 \pm 0.015$ hours, and a period of $P = 3.5239 \pm 0.0003$ days. The fitted duration in our model is slightly unreliable since data covering the egress of the transit is missing on most nights (see Figure 7).

The range of periods over which a transit search can be conducted depends upon the sampling and duration of the survey. In particular, large gaps in the sampling can lead to cycle-count ambiguity since n unobserved transits may have occurred during the gaps. This is clear from the periodogram shown in Figure 9 which shows aliases that differ from the real period by 1 cycle per 7 days. Figure 9 also contains a frequency plot which shows that the alias periods are equally spaced by 1 cycle per 7 days.

5.4 Transit-like Events and Variable Stars

The monitoring program of WASP0 is ideal for detecting many kinds of stellar variability. As a result, the Pegasus field data have yielded lightcurves of stars whose variable nature was previously unknown. Shown in Figure 10 are four examples of stars in the field which exhibit variable behaviour identified by the transit detection algorithm. Clearly each of these stars are either too deep or too variable to be a genuine planetary transits and are likely to be eclipsing or grazing eclipsing binaries. A comprehensive study of

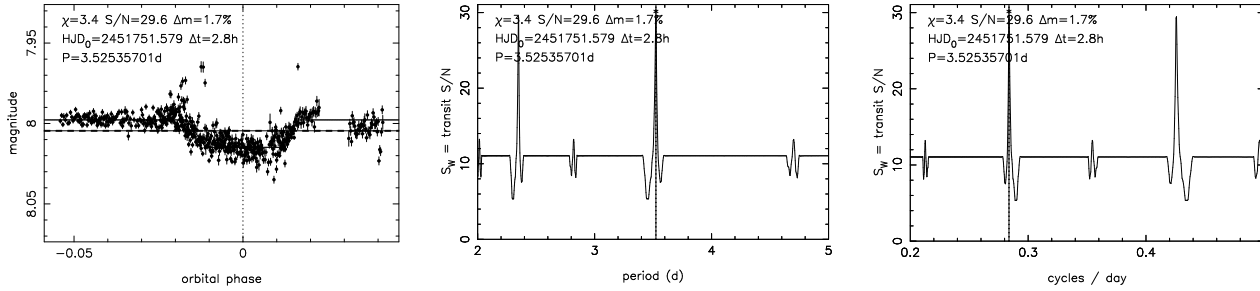


Figure 9. Results of a refined transit model fit to the data obtained of HD 209458. The left panel shows the folded data with the best fit model. The middle panel shows the periodogram from a period sweep ranging from 2 to 5 days. The right panel is a frequency plot which shows the number of cycles/day.

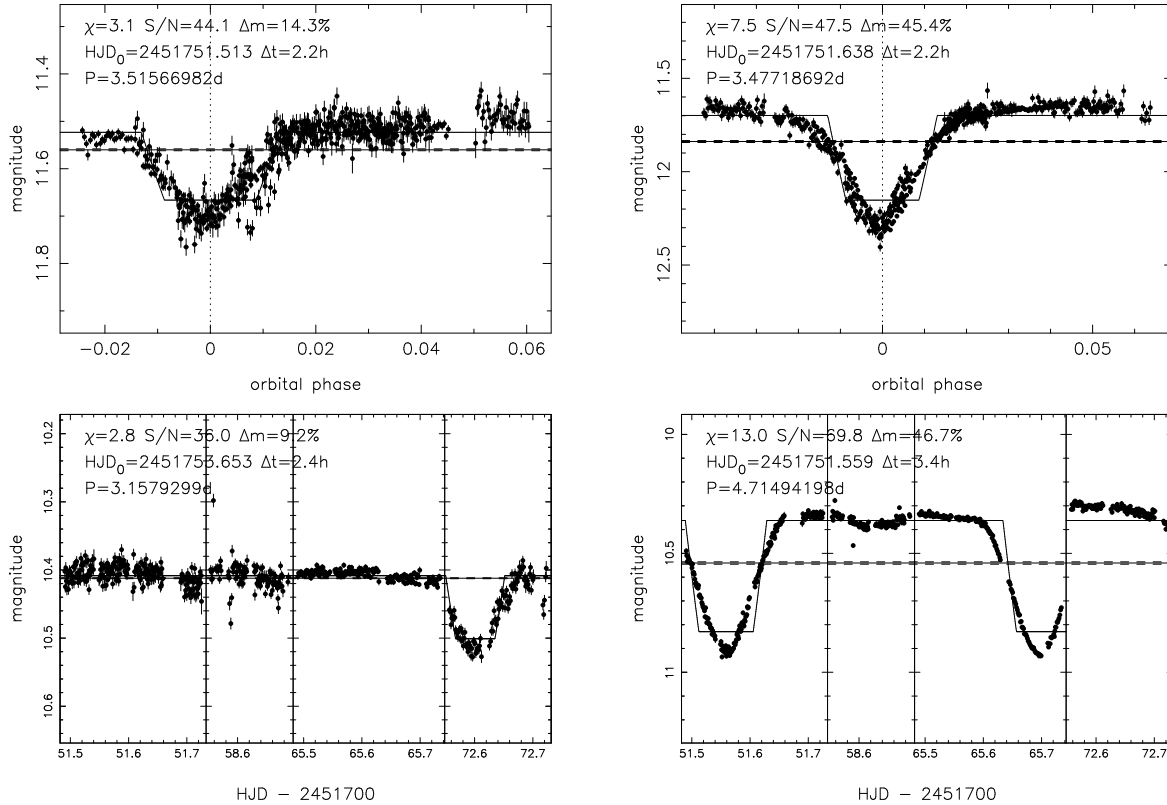


Figure 10. Four example stars exhibiting transit-like or variable behaviour. The top two panels are show folded lightcurves and the bottom two panels are unfolded.

new variable stars discovered in the Pegasus field will be published elsewhere.

6 CONCLUSIONS

We have described an inexpensive prototype survey camera designed to monitor a wide-field on-sky area and hunt for transiting extra-solar planets. Large datasets have so far been obtained of fields in Draco and Hyades with some additional nights monitoring Pegasus at predicted transit times of the known extra-solar planet HD 209458b. A pipeline has been developed which makes use of the Tycho-2 and USNO-B catalogue to provide an astrometric solution for

each frame. The transformed source list is then used to perform weighted aperture photometry at the location of each object in the catalogue.

The resulting analysis of WASP0 Pegasus data presented here demonstrates that this instrument is able to achieve millimag photometry and hence the necessary precision required to detect transit events due to extra-solar planets. A transit detection algorithm has been described and has shown that it is effective at extracting stars with exhibit transit-like behaviour from the bulk of the dataset.

It is unfortunate that the WASP0 camera only observed using a clear filter. This means that multi-colour follow-up observations of transit candidates, needed to dis-

tinguish other possible physical scenarios, will be required to be sought after elsewhere.

This prototype has successfully served as a proof-of-concept for SuperWASP, a robotically operated, multi-camera instrument recently constructed on La Palma. The primary science goal of the SuperWASP project is to use the well-sampled lightcurves to detect planetary transits, but the data will also be used to detect Near-Earth Objects and optical transients.

ACKNOWLEDGEMENTS

The authors would like to thank Aleksander Schwarzenberg-Czerny for useful discussions regarding the transit detection algorithm. The authors would also like to thank PPARC for supporting this research and the Nichol Trust for funding the WASP0 hardware.

REFERENCES

- Bertin, E., Arnouts, S., 1996, *A&AS*, 117, 393
Borucki, W.J., Scargle, J.D., Hudson, H.S., 1985, *ApJ*, 291, 852
Borucki, W.J., Caldwell, D., Koch, D.G., Webster, L.D., Jenkins, J.M., Ninkov, Z., Showen, R., 2001, *PASP*, 113, 439
Charbonneau, D., Brown, T.M., Latham, D.W., Mayor, M., 2000, *ApJ*, 529, L45
Delfosse, X., Forveille, T., Mayor, M., Perrier, C., Naef, D., Queloz, D., 1998, *A&A*, 338, L67
DeFavä, C., Deleuil, M., Barge, P., 2001, *A&A*, 365, 330
Doyle, L.R., et al., 2000, *ApJ*, 535, 338
Henry, G.W., Marcy, G.W., Butler, R.P., Vogt, S.S., 2000, *ApJ*, 529, L41
Høg, E., et al., 2000, *A&A*, 355, L27
Kovács, G., Zucker, S., Mazeh, T., 2002, *A&A*, 391, 369
Lineweaver, C.H., Grether, D., 2003, *ApJ*, 598, 1350
Marcy, G., Butler, R., 1996, *ApJ*, 464, L147
Mayor, M., Queloz, D., 1995, *Nat*, 378, 355
Monet, D.G., et al., 2003, *ApJ*, 125, 984
Schechter, P.L., Mateo, M., Saha, A., 1993, *PASP*, 105, 1342
Street, R.A., et al., 2003, *ASP Conf. Series*, Vol. 294, *Scientific Frontiers in Research on Extrasolar Planets*, eds. D. Deming & S. Seager, p. 405